The first-order phase transition and colossal magnetoresistance effects in bulk Gd-doped $La_{0.67}Sr_{0.33}MnO_3$

XUGAO CUI*, XIUKUN HU, HONGXU XIA, JIANGYING YU, DUNHUI WANG, SHIYUAN ZHANG
National Laboratory of Solid State Microstructures, Department of Physics, Nanjing University, Nanjing 210093, People's Republic of China
E-mail: cuixugao@nju.org.cn

Considerable attention has been paid to perovskite-like manganites $R_{1-x}A_xMnO_3$ (where R = La, Pr, Y, etc. and A = Ca, Sr, Ba, etc.) owing to their colossal magnetoresistance (CMR) and other novel properties [1–4]. In these ABO_3 perovskite-like mangnites, the average ionic radius of the A site $\langle r_A \rangle$ plays a very important role [5]. The Mn–O–Mn bond angle (deviation from 180°) in these compounds changes with the variation of $\langle r_A \rangle$, which affects the transfer interaction of the e_g conduction electrons (holes) at Mn^{3+} with $t_{2g}^3 e_g^1$ configuration. Hwang *et al*. [6] have systematically studied the effects of $\langle r_A \rangle$ on the Curie temperature, resistivity and CMR in the $(La_{1-y}Pr_y)_{0.7}Ca_{0.3}MnO_3$ and $La_{0.7-y}Y_yCa_{0.3}MnO_3$ system by changing $\langle r_A \rangle$ while keeping the Mn^{+3}/Mn^{+4} ratios fixed at 7/3. They found that with decreasing $\langle r_A \rangle$, and significant MR occurs at lower temperatures with increasing thermal hysteresis, and the magnitude of the MR increases dramatically. Furthermore, with the decrease of the average ionic radius of the A site $\langle r_A \rangle$, the samples usually transit from large-bandwidth manganites to low-bandwidth manganites and the tendencies of phase separation (PS) on ferromagnetic (FM)/metal clusters and antiferromagnetic (AFM)/insulator clusters are enhanced [7]. When a magnetic field is applied upon to samples with mixed-phase state, FM clusters grow in size and volume in the AFM background, as observed in the sample of $(La_{1-y}Pr_y)_{0.7}Ca_{0.3}MnO_3$ by Uehara *et al*. 8]. This field-induced transition is associated with a high-to-low-volume transition and the transition should be of first order [7]. Furthermore, it is well known that the first-order-phase transition is often responsible for the large magnetostriction (MS) [2]. However, the relevant report is not adequate.

In this article, we report a large volume-magnetostriction (VMS) of -135×10^{-6} in a magnetic field of 1 T at 115 K in $(La_{0.45}Gd_{0.55})_{0.67}Sr_{0.33}MnO_3$, accompanied by a first-order-like ferromagnetic transition, and a CMR of −1840% in a magnetic field of 4 T at 118 and try to discuss the origin of the VMS in this sample.

We prepared polycrystalline samples of $(La_{1-x}Gd_x)_{0.67}Sr_{0.33}MnO_3$ (LGSMO) with $x = 0.1, 0.2, 0.3, 0.4, 0.5, 0.55, 0.6, 0.7$ by conventional solid-state reaction method. Appropriate amounts of high-purity Nd_2O_3, $SrCO_3$, Gd_2O_3 and Mn_3O_4 powders were mixed and presintered at 900 °C for 10 hr in air. After that, they were ground, pressed into disks, then sintered at 1250 °C for 50 hr in air. The resistivity (ρ) were measured by the standard DC four-probe technique using a Model-6000 physical property measurement system (PPMS). The MR is defined as $((\rho_H - \rho_0)/\rho_H) \times 100\%$, where ρ_H, ρ_0 are the resistivities in the fields of H and zero, respectively. The temperature dependence of the magnetizations of the samples was measured by vibrating sample magnetometer (VSM, LakeShore). X-ray diffraction (XRD) with the Cu $K\alpha$ radiation was adopted to characterize the structure of the samples. The MS was measured by strain gauge attached to the samples. The VMS (ω) and linear-magnetostriction (LMS) (λ) were calculated from the formulas $\omega = \lambda_{//} + 2\lambda_t$ and $\lambda = \lambda_{//} - \lambda_t$, where $\lambda_{//}$ and λ_t are the results of MS measured parallel and perpendicular to the applied field.

Fig. 1 shows XRD patterns of the selected samples with $x = 0.3, 0.55, 0.7$. For the $x = 0.3$ sample, the phase-structure is typical of rhombohedral ($R\bar{3}c$ space group), which is in good agreement with earlier literature [8]. Comparing (a), (b) and (c), we can see that the diffraction peak shifts to higher 2θ angle with the increase of x, for example, the (202) peak in Fig. 1c shifts to higher 2θ angle in comparison with the 2θ angle position of the (101) and (104) peak in Fig. 1a, which indicates the decrease of the c-axis lattice constant. It is because the radius of Gd^{3+} (∼1.11 Å) is less than that of La^{3+} (∼1.22 Å), which results in the decrease of the average radius of A-site with the increase of x. The shift in oxygen positions of samples is very important in this structural phase change but this shift is random, unlike the regular shift to higher 2θ angle with the increase of x in Fig. 1. In the $x < 0.55$ region, the structure remains rhombohedral, when $x > 0.55$, it transforms to OF and we can see it is completely orthorhombic at $x = 0.7$ from Fig. 1c. The transitional region is $x \cong 0.55$ and the XRD patterns of the $x = 0.55$ sample is shown in Fig. 1b.

The Curie temperature (T_c) as a function of Gd content is plotted in Fig. 2. T_c is obtained by measuring the temperature-dependence of the magnetizations in an applied field of 100 Oe. The typical temperature-dependence of the magnetization is shown in the inset of Fig. 2. From the Fig. 2, we can see that T_c decreases

* Author to whom all correspondence should be addressed.

0022-2461

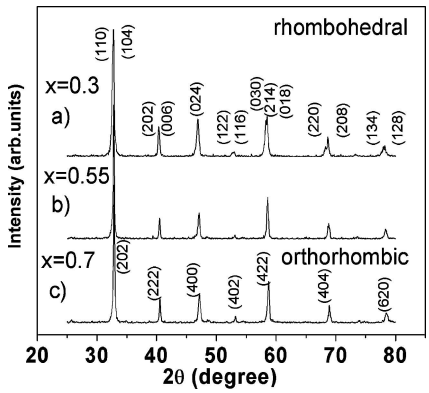

Figure 1 XRD patterns of (a) $x = 0.3$, (b) $x = 0.55$, and (c) $x = 0.7$ samples.

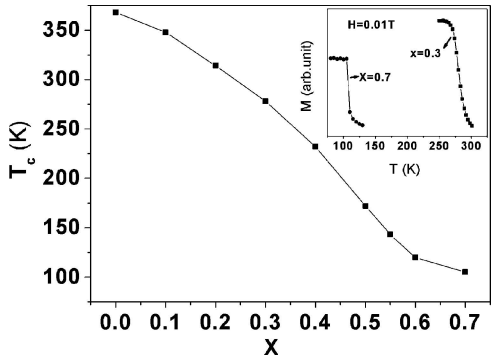

Figure 2 The Curie temperature (T_c) as a function of Gd content (x). The typical temperature-dependence of the magnetization is shown in the inset.

monotonously with the increase of the Gd content. This is in agreement with the report by Hwang *et al.* [6]. Another possible cause that leads to the fluctuation of T_c is the concentration of oxygen in LGSMO samples. However, the fluctuation of T_c can not affect the overall tendency in the decrease of T_c of the LGSMO samples. The coercivities of the samples (except $x = 0.7$) at 115 K are all ~70 Oe. The *M–H* hysteresis loops at $T = 115$ K are not shown here.

The temperature-dependence of resistivity in zero field for the $x = 0.3$, 0.55, 0.7 is shown in Fig. 3. The inset is the temperature-dependences of MR. The applied magnetic field are 0.8 T and the samples were cooled by liquid nitrogen in this low magnetic field and zero fields. The $x = 0.3$, 0.55 samples both un-

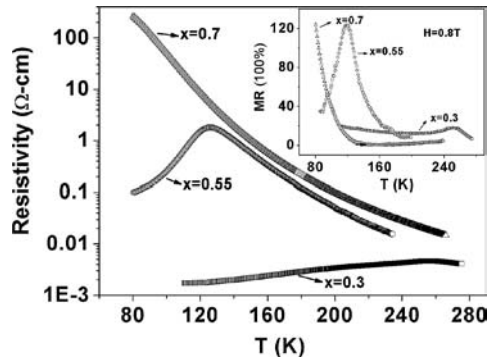

Figure 3 The temperature-dependence of resistivity in zero field for the $x = 0.3$, 0.55, 0.7 samples. The inset is the temperature-dependences of MR.

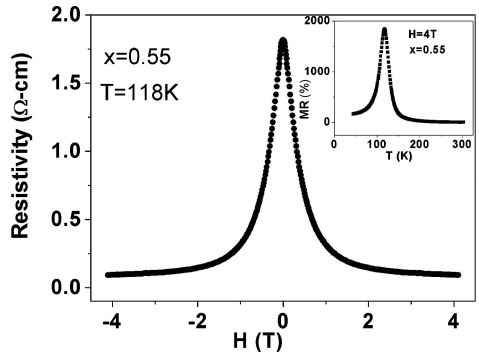

Figure 4 The isotherm of resistivity for the $x = 0.55$ sample at 118 K. The inset is the temperature-dependence of MR for this sample.

dergo a transition from semiconductor-like to metal in the process of temperature-cooling with a maximum resistivity. We define the temperature at which samples transit from semiconductor-like to metal as T_p. But for the $x = 0.7$ sample, this transition from semiconductor-like to metal occurs below the temperature of liquid nitrogen and can not be observed. From Fig. 3, we can see also that with the increase of x, the resistivity at T_p and MR effect increases dramatically and the T_p shifts to low temperature. This phenomenon has been interpreted as a gradual bending of the Mn–O–Mn bond with decreasing $\langle r_A \rangle$, which causes the enhancement of the carrier effective mass or the narrowing of the band width (from a large-bandwidth manganite with $x = 0$ to a low-bandwidth manganite with $x \geq 0.55$) and a reduction of the mobility of the electrons (holes) [6, 9]. Fig. 4 shows the isotherm of resistivity at 118 K for the $x = 0.55$ sample. The inset is the temperature-dependence of MR for the $x = 0.55$ sample. Liquid helium was used to cool samples for the measurement of MR in a higher magnetic field of 4 T. From Fig. 4, the initial drop of resistivity both originates from extrinsic MR effect that occurs at grain boundaries and intrinsic MR effect governed generally by double-exchange (CMR). Hwang *et al.* [10] and Gupta *et al.* [11] found that the low-field extrinsic MR effects are usually significantly larger than the low-field intrinsic MR effects in various magnetic oxides. With field increasing, the magnetization is saturated and the magnetic moments are aligned, the drop of resistivity is mainly contributed by CMR. From Fig. 4, the drop of resistivity is not completely saturated up to 4 T and the MR is −1840% in the magnetic field of 4 T at 118 K.

The VMS in a 1 T field at room-temperature for the $x = 0.1$, 0.2, 0.3, 0.4, 0.5, 0.55, 0.6, 0.7 is -6×10^{-6}, -30×10^{-6}, -2×10^{-6}, 0, 0, 0, 0, 0, respectively. The isotherms of MS at 115 K for the $x = 0.55$ sample is shown in Fig. 5. Comparing the $\lambda_{//}$ and λ_t, we can see that the MS for this sample shows the anisotropic behavior ($\lambda_{//} \neq \lambda_t$). For the $x = 0.3$, 0.5 and 0.6 samples, $\lambda_{//}$ and λ_t have the opposite sign (not shown here). But for the $x = 0.55$ sample, $\lambda_{//}$ and λ_t are both negative, which means that it contracts simultaneously in both directions parallel and perpendicular to the field. This leads to a very large VMS for the $x = 0.55$ sample when a field was applied upon to it. We can also observe hysteresis of MS against changes in the magnetic field for the $x = 0.55$ sample, which is characteristic of the

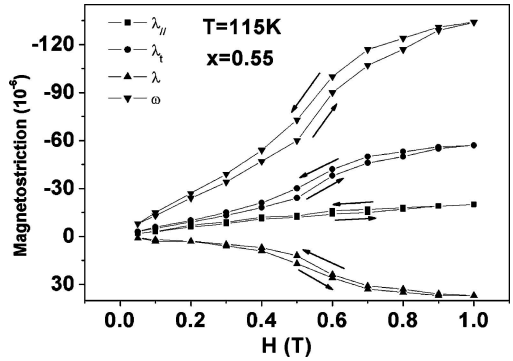

Figure 5 The isotherms of MS of the $x = 0.55$ sample.

first-order phase transition [2]. But for the $x = 0.3$, 0.5, 0.6 samples, hysteresis can't be observed. For the $x = 0.55$ sample, with increasing the magnetic field the VMS increases gradually when $H < 0.5$ T, but in the range of field about $0.5\ T < H < 0.6$ T, the VMS increases dramatically, and then becomes gradual again when $H > 0.6$ T up to -135×10^{-6} at 1 T. The VMS in the $x = 0.55$ sample is much greater than that in the $x = 0.2$ sample. This phenomenon can be related to the structural phase transition. With x increasing, the samples transit from $La_{0.67}Sr_{0.33}MnO_3$ ($x = 0$, the large-bandwidth manganite) to $Gd_{0.67}Sr_{0.33}MnO_3$ ($x = 1$, the low-bandwidth manganite) and the PS tendencies in samples are enhanced [7]. As a result, the MR effect, resistivity increase and the T_c is lowered. In the $x = 0.55$ sample, there exist two competitive phases of low-volume metallic FM clusters with delocalized carriers and high-volume insulating A-type AFM clusters with delocalized carriers due to the strong s–d exchange [7, 12]. With the increase of the magnetic field applied upon to the $x = 0.55$ sample, the FM clusters grow in both size and volume and the AFM clusters degenerate in this sample [9]. This causes CMR and large MS effects. Furthermore, this transition is of first order [7]. It is clear that in Fig. 5, the ω and λ show hysteresis at 115 K temperature against changes in the magnetic field. Therefore, we conclude the CMR and large VMS for the $x = 0.55$ sample could be attributed to the first-order structural phase transition from metallic FM to the A-type AFM phase.

In summary, we have investigated the phase-structure and MR, MS effects in bulk polycrystalline LGSMO samples. We find that with increase of x in the samples, the phase-structure transforms from RF to OF with a critical point $x = 0.55$. At the same time, T_c declines rapidly and MR, resistivity of the samples increases. At $x = 0.55$, the phase-structure is of mixed-phase state and the applied magnetic field can move high-volume insulating A-type AFM clusters to the phase of low-volume metallic FM clusters. In the $x = 0.55$ sample, the maximum VMS is -135×10^{-6} in a magnetic field of 1 T at 115 K, and the maximum MR is -1840% in the magnetic field of 4 T at >118 K.

Acknowledgment

This work is supported by Special Funds for Major State Basic Research Project of China under Grant No. 2001CB610603.

References

1. R. M. KUSTERS, J. SINGLETON, D. A. KEEN, R. MCGREEVY and W. HAYES, *Physica* B **155** (1989) 362.
2. H. KUWAHARA, Y. TOMIOKA, Y. MORITOMO, A. ASAMITSU, M. KASAI, R. KUMAI and Y. TOKURA, *Science* **271** (1996) 80.
3. K. CHAHARA, T. OHNO, M. KASAI, and Y. KOZONO, *Appl. Phys. Lett.* **63** (1993) 1990.
4. G. C. XIONG, Q. LI, H. L. JU, R. L. GREENE and T. VENKATESAN, *Appl. Phys. Lett.* **66** (1995) 1689.
5. J. B. GOODENOUGH and J. M. LANGO, Landolt-Boornstein Tabellen, New series (Springer, Berlin, 1970), Vol III/4a.
6. H. Y. HWANG, S.-W. CHEONG, P. G. RADAELLI, M. MAREZIO and B. BATLOGG *Phys. Rev. Lett.* **75** (1995) 914.
7. E. DAGOTTO, T. HOTTA and A. MOERO *Phys. Rep.* **344**, (2001) 1.
8. M. UEHARA, S. MORI, C. H. CHEN and S. −H. CHOENG, *Nature* **399** (1999) 560.
9. URUSHIBARA, Y. MORITOMO, T. ARIMA, A. ASAMITSU, G. KIDO and Y. TOKURA *Phys. Rev.* B **51** (1995) 14103.
10. J. FONTCUBERTA, B. MARTÍNEZ, A. SEFFAR, S. PINOL, J. L. GARCÍA-MUNOZ and X. OBRADORS *Phy. Rev. Lett.* **76** (1996) 1122.
11. H. Y. HWANG, S.-W. CHEONG, N. P. ONG and B. BATLOGG *Phys. Rev. Lett.* **77** (1996) 2041.
12. GUPTA, G. Q. GONG, G. XIAO, P. R. DUNCOMBE, P. LECOEUR, P. TROUILLOUD, Y. Y. WANG, V. P. DRAVID and J. Z. SUN *Phys. Rev.* B**54** (1996) R15629.
13. E. L. NAGAEV, *Phys. Rep.* **346** (2001) 381.

Received 14 December 2004
and accepted 19 April 2005